

Achromatic linear retarder with tunable retardance

ABDELGHAFOUR MESSAADI¹, MARÍA M. SÁNCHEZ-LÓPEZ^{2,*}, ASTICIO VARGAS³,
PASCUALA GARCÍA-MARTÍNEZ⁴, IGNACIO MORENO¹

¹Departamento de Ciencia de Materiales, Óptica y Tecnología Electrónica, Universidad Miguel Hernández, 03202 Elche, Spain.

²Instituto de Bioingeniería, Depto. de Física y Arquitectura de Computadores, Universidad Miguel Hernández, 03202 Elche, Spain.

³Departamento de Ciencias Físicas, Universidad de La Frontera, Temuco, Chile.

⁴Departament d'Òptica, Universitat de València, 46100 Burjassot, Spain.

*Corresponding author: mar.sanchez@umh.es

Received XX Month XXXX; revised XX Month, XXXX; accepted XX Month XXXX; posted XX Month XXXX (Doc. ID XXXXX); published XX Month XXXX

We present a universal design and proof-of-concept of a tunable linear retarder of uniform-wavelength response in a broad spectral range. It consists of two half-wave retarders (HWR) in-between two quarter-wave retarders (QWR), where the uniform retardance can be tuned continuously by simply rotating one of the HWRs. A proof-of-concept of this design is built by using commercially available Fresnel rhomb retarders (FR) that provide retardation with almost wavelength-uniformity in the visible and near infrared from 450 to 1550 nm. The design is universal since other achromatic QWR and HWR could also be employed. The system is experimentally demonstrated to control the state of polarization of a supercontinuum laser. © 2018 Optical Society of America

OCIS codes: (260.5430) Polarization; (120.2130) Ellipsometry and polarimetry;

<http://dx.doi.org/10.1364/OL.99.099999>

Precision spectral control of polarization is an important subject for many applications such as spectro-polarimetry, optical communications, biomedical optical imaging, military target identification, chemical analysis, and remote sensing [1]. Designers generally choose wave-plates to alter or analyze the state of polarization (SOP), and different types of retarders exist that suit different applications [2]. They are usually spatially uniform retarders, but recent technological advances have made possible to fabricate spatially patterned retarders, becoming the basis of new optical elements based on the geometrical phase [3].

Usually, retarders are made of birefringent materials. They inherently suffer from dispersion, and their retardance typically depends strongly on the wavelength [4]. In order to avoid dispersion, different techniques have been reported to fabricate retarders with weak wavelength-variation. This is usually achieved by cascading standard HWR and QWR plates with appropriate orientation of their principal axis. The number of elements is

determined by the degree of requested achromaticity and spectral range. The wider the spectral range, the more layers are required for good performance [5-12]. Recent designs also include the plates's thickness as a parameter [13] to achieve high achromaticity. With these designs, large polarization control was demonstrated in the visible and near infrared spectrum [11,12]. Other approaches use structural birefringence of subwavelength gratings to fabricate achromatic polarization rotators [14,15].

Composite retarders of any desired retardation can be designed, although only HW and QW achromatic retardance has been shown experimentally in a broad spectral range. Changing the target retardance implies redesigning the system, that is, recalculating the azimuth orientations (or also the thickness) of each element in the stack. This makes difficult to tune the retardance of these achromatic composite retarders.

Liquid-crystal (LC) technology offers tunable retardance upon an applied voltage. However, LC devices are typically made of a single anisotropic layer, thus far from being wavelength compensated. A combination of LC retarders to create a tunable achromatic retarder was reported [16], where the retardance of each layer can be changed to yield a tunable achromatic retarder. However, this approach was demonstrated with only two LC retarders, and therefore the operating spectral range is relatively narrow.

Another approach was proposed [17], where the light beam is spatially dispersed and then projected onto a LC spatial light modulator, with adjustable applied voltage at every pixel according to the incident wavelength. The light reflected back is then recombined, so the complete system acts as a programmable retarder where the spectral retardance can be controlled at will. For instance, it can be adjusted to provide a constant retardance in the complete operating wavelength range. However, it is a complex optical system, with important losses.

Here a simpler approach is adopted based on cascading two HWRs in between two QWRs. This simple optical system acts as a linear retarder of arbitrary retardance tunable by simply rotating one of the HWRs. This universal design can be implemented by either composite achromatic waveplates [5,11,13] or Fresnel rhombs (FR) as achromatic retarders.

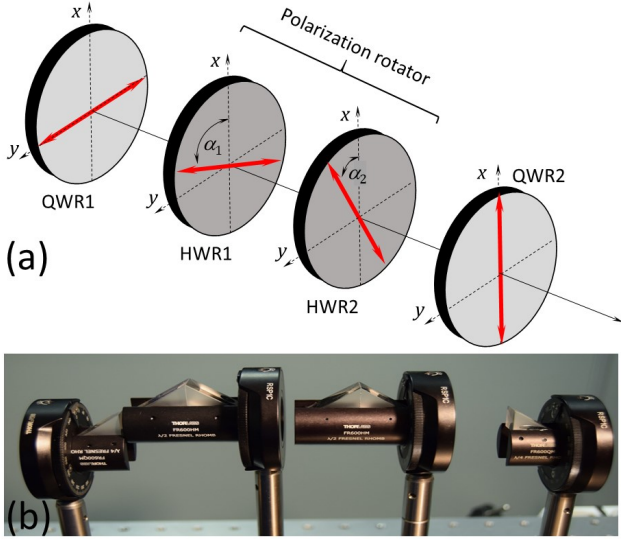


Fig. 1. (a) Linear retarder system of tunable retardance equal to $4(\alpha_1 - \alpha_2)$. Experimental implementation with Fresnel rhombs.

Figure 1(a) shows a scheme of the proposed optical set-up, which is described in two steps. First, the combination of two achromatic HWRs to create a polarization rotator with a rotation angle that does not depend on wavelength. If α_1 and α_2 denote the orientation of each HWR with respect to the laboratory axis, the rotation angle of this polarization rotator is given by $2(\alpha_2 - \alpha_1)$ and can be varied simply by changing the relative orientation between the two HWRs. Then, the polarization rotator is inserted between two achromatic QWRs. If the HWRs and QWRs that constitute the system are achromatic, the setup acts as a retarder with uniform retardance (within the limits imposed by the degree of achromaticity of the individual retarders), and the retardance value, $4(\alpha_1 - \alpha_2)$, can be adjusted by merely rotating one of the HWRs.

We use FRs to build a proof-of-concept of this universal design. FRs are not birefringent retarders. Instead, their retardance is based on the phase shift between TE and TM modes upon total internal reflection [18-20]. And this phase shift is almost uniform over a very wide spectral range. This is the case, for instance, when building polarization conversion mirrors [21,22]. Nevertheless, FRs are not perfectly achromatic; wavelength, incident angle and transmission errors have been reported [18,23].

Figure 1(b) shows a picture of the experimental system. It is composed of two FR-HWRs (model FR600HM) and two FR-QWRs (model FR600QM), all from Thorlabs; and with wavelength operating range 400-1550 nm. Two Glan-Taylor linear polarizers from Edmund Scientific operating in the 350-2200 nm range, are placed at the input and output of the system. Since light impinges with normal incidence, any in-plane rotation of the FR-HWRs does not alter the direction of the emerging beam, so they can be rotated without realigning the system. On the contrary, FR-QWRs deviates laterally the emerging light compared to the input direction [18]. This is why, we place the first FR-QWR (Fig. 1(b)) vertically oriented, instead of horizontally. This change does not affect the basic performance, as it will be discussed later.

We use a supercontinuum laser light source (FYLA-SC500), which emits a broadband spectrum from 450 to 2400 nm. The system's output is captured by an optical fiber and is directed to a spectrometer (Stellar-Net, STN-BLK-C-SR) which measures the

spectrum in the 200-1080 nm range with a resolution of 2 nm, and to another spectrometer (Stellar-Net, STE-RED-WAVE-NIR-512-25) that measures from 900 to 1550 nm with a resolution of 3 nm.

Using the Jones matrix formalism the polarization rotator system in Fig. 1(a) is described by

$$\mathbf{HWR}(\alpha_2) \cdot \mathbf{HWR}(\alpha_1) = \mathbf{R}(2(\alpha_1 - \alpha_2)) \quad (1)$$

where, $\mathbf{HWR}(\alpha) = \mathbf{R}(-\alpha) \cdot \mathbf{HWR}(0) \cdot \mathbf{R}(\alpha)$ is the Jones matrix of a HWR with orientation α , and $\mathbf{HWR}(0) = \mathbf{diag}(1, -1)$. We assume the x axis aligned with the laboratory vertical direction. The rotation matrix is given by

$$\mathbf{R}(\alpha) = \begin{pmatrix} \cos(\alpha) & \sin(\alpha) \\ -\sin(\alpha) & \cos(\alpha) \end{pmatrix}. \quad (2)$$

Equation (1) shows that cascading two HWRs results in a polarization rotator with a rotation angle equal to twice their relative angle. Thus, considering the FR almost wavelength-independent retardance, we build a polarization rotator with a uniform wavelength response using two FR-HWRs.

The probe of such polarization rotator is given in Fig. 2. The input and output polarizers are both considered oriented at angles $\theta_1 = \theta_2 = 0^\circ$. The first rhomb is oriented at $\alpha_1 = 0^\circ$, but the second rhomb's orientation (α_2) varies from 0° to 45° . Therefore, the polarization rotator should rotate the input polarization by $2\alpha_2$ for all wavelengths and the transmitted spectrum should keep its shape upon varying α_2 , whilst decreasing according to Malus law by $\cos^2(2\alpha_2)$ uniformly for all wavelengths. A relative transmission of 100%, 75%, 50% and 25% is expected for $\alpha_2 = 0^\circ, 15^\circ, 22.5^\circ$ and 30° . And light should be completely extinguished for all wavelengths when $\alpha_2 = 45^\circ$, when the 90° polarization rotator is generated. However, as mentioned earlier, FRs do present limited achromaticity, which must be taken into account when cascading them [18]. The manufacturer provides the FR retardance at six specific wavelengths in the 400-1550 nm range [24], being the overall retardance variation 2.99° for the FR-QWR and 5.97° for the FR-HWR. Using these data we obtain a retardance curve versus wavelength that we use in numerical simulations.

Figures 2(a)-(d) show the calculated transmissions considering a flat input spectrum, where each panel corresponds to $\alpha_2 = 15^\circ, 22.5^\circ, 30^\circ$ and 45° , respectively. The effect of the FRs retardance dispersion on the polarization rotator is retrieved from the difference between the simulated transmittance $I_{sim}(\lambda)$ and a target transmittance I_0 (assuming perfect achromatic FRs) through the quadratic relative error (QRE) $\varepsilon(\lambda) = \sqrt{(I_{sim}(\lambda) - I_0)^2}$. The

average QRE $\langle \varepsilon \rangle$ in the 450-1550 nm range appears on each panel. From these low QREs, the achromatic performance of this proof-of-concept polarization rotator seems excellent.

Figure 2(e) displays the system's experimental transmission captured by the two spectrometers in the range from 450 to 1550 nm. Note the narrow dark band around 1064 nm, since we filtered the high-power peak of the supercontinuum laser. The figure shows the progressive decrease of the transmitted spectrum, with a maximum transmission for $\alpha_2 = 0^\circ$. The inset shows the expected output polarizations, drawn in the color of the corresponding transmission curve. The figure includes simulations (solid curves) obtained after multiplying the curves in panels (a) to (d) by the supercontinuum light spectrum $I_s(\lambda)$ (top curve in panel 2(e)).

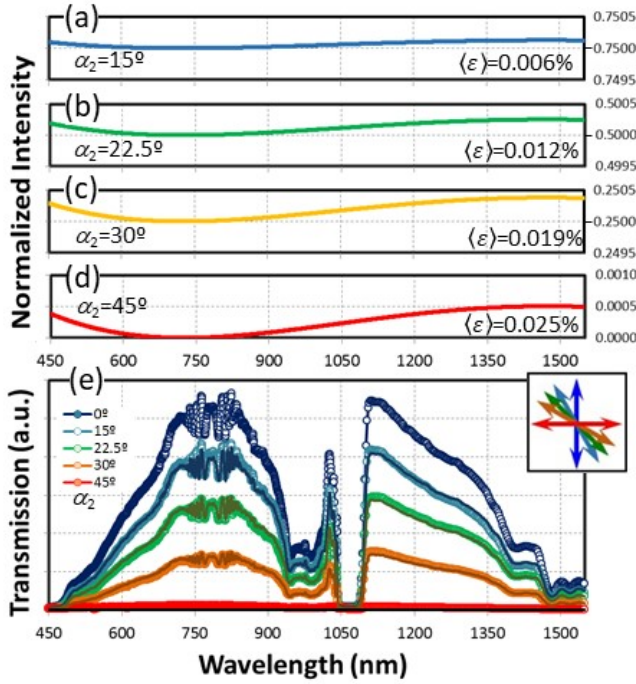


Fig. 2. Spectral transmission of the polarization rotator built with FRs. $\alpha_1=0^\circ$ and various orientations α_2 are considered. Polarizers are oriented at $\theta_1=\theta_2=0^\circ$. (a)-(d) Simulated transmission considering the FR retardance dispersion and a flat input spectrum for the given α_2 . (e) Experimental transmission and simulation considering the spectrum of the light source.

They agree well with the experimental curves. However, in order to account for other weaknesses of the FRs that may affect the experimental errors (like acceptance angle and transmission errors due to non-perfectly aligned components [18]), we evaluate the experimental QRE defined as $\varepsilon'(\lambda) = \sqrt{(I_{exp}(\lambda) - I_{sim}(\lambda))^2} / I_S(\lambda)$, where $I_{exp}(\lambda)$ is the measured spectrum. The average value $\langle \varepsilon' \rangle$ is computed for each orientation α_2 . These errors are two orders of magnitude larger than those in panels (a-d); namely, $\langle \varepsilon' \rangle = 3.6\%$, 4.0% , 4.5% and 7.3% . Nevertheless, we can say Fig. 2(e) shows a proof-of-concept of a λ -independent polarization rotator.

Let us now discuss the tunable linear retarder. For that purpose, we use a solution inverse to that in [25,26]. In these works, a LC linear tunable retarder was converted into a polarization rotator by placing it between two QWRs oriented at $\pm 45^\circ$ with respect to the LC director. Here we place two QWRs on the extremes of our polarization rotator, in order to transform it into a linear retarder. Using the Jones formalism, the system in Fig. 1 is described by:

$$\mathbf{M} = \mathbf{QWR}(0) \cdot \mathbf{R}(2(\alpha_1 - \alpha_2)) \cdot \mathbf{QWR}(90^\circ) = \begin{pmatrix} \cos(\phi/2) & -i \sin(\phi/2) \\ -i \sin(\phi/2) & \cos(\phi/2) \end{pmatrix} \quad (3)$$

where $\mathbf{QWR}(\alpha) = \mathbf{R}(-\alpha) \cdot \mathbf{QWR}(0) \cdot \mathbf{R}(+\alpha)$ and $\mathbf{QWR}(0) = \mathbf{diag}(1, i)$. This matrix corresponds to a linear retarder of retardance $\phi = 4(\alpha_1 - \alpha_2)$ oriented at 45° , namely:

$$\mathbf{M} = \mathbf{R}(-45^\circ) \cdot \begin{pmatrix} e^{-i\phi/2} & 0 \\ 0 & e^{+i\phi/2} \end{pmatrix} \cdot \mathbf{R}(+45^\circ). \quad (4)$$

Note that in the experimental realization in Fig. 1(b) the two FR-HWRs that constitute the polarization rotator must be moved up in order to be centered on the new height of the beam. Note also that the first QWR is not oriented correctly, since it is rotated by 90° . However, a QWR rotated by 90° is equivalent to the aligned QWR preceded by an aligned HWR. Therefore, we can consider the experimental system described by the product $\mathbf{M} \cdot \mathbf{HWR}(0)$. For practical purposes using FRs, this extra retarder could be compensated with another FR-HWR located at the input of the system. However, in order to avoid an additional element, we simply took into account the change in polarization induced by this extra HWR element. If the input polarization is linear and vertically or horizontally oriented, this extra HWR has no influence at all.

The probe of such tunable retarder is given in Fig. 3. We keep the input polarizer at $\theta_1=0^\circ$, i.e., with an angle of 45° with respect to the neutral axes of the equivalent retarder system. Now, a change in the retardance of the composed retarder system changes the ellipticity of the emerging polarization, while keeping the azimuth constant. Figure 3(a) shows the expected transmission for a flat input spectrum when the output polarizer is at 45° (keeping the input polarization at 0°) and for three values of α_2 . If $\alpha_2=0^\circ$ no retardance is introduced and half of the input intensity is transmitted in the whole spectral range. When $\alpha_2=22.5^\circ$ the system should behave as an achromatic QWR, thus generating circularly polarized light. Consequently, the transmission function should be again a flat line of value 0.5. However, this only occurs around 750 nm (were the FR retardance is perfectly 90°) and from this wavelength the curve deviates from the ideal value due to the FR retardance dispersion. The curve when $\alpha_2=11.25^\circ$ lies in between the former cases, with a lower effect of the FR dispersion.

Figures 3(b), 3(c) and 3(d) show the experimental results and the corresponding numerical simulations (solid lines) for $\alpha_2=0^\circ$, 11.25° and 22.5° respectively. In each figure, the blue, green and red lines denote the transmission when the output polarizer is oriented at $\theta_2=0^\circ$, 45° and 90° respectively. By rotating this analyzer we check the expected emerging state of polarization, which is drawn in the inset. Because the system employs four cascaded FRs, experimental errors are expected. We again account for these effects by computing the experimental average QRE $\langle \varepsilon' \rangle$ previously defined, which is displayed in each panel.

In Fig. 3(b) the retardance is zero, and light emerges linearly polarized. This is clearly shown by the total extinction achieved when the analyzer is oriented at 90° . This not the case in Fig. 3(c), where the retardance of the equivalent system is $\phi=45^\circ$. The expected output polarization is now elliptical. The minimum transmission is achieved for $\theta_2=90^\circ$, showing that the orientation of the polarization ellipse remains vertical, but a total extinction is not achieved. Finally, Fig. 3(d) shows the case when $\alpha_2=22.5^\circ$ (retardance $\phi=90^\circ$). Now the system operates as a QWR and thus the emerging state is a broadband circularly polarized light beam. This is verified by the overlapping of all curves upon rotating the analyzer. In all cases the shape of the spectral curve is kept, showing that the polarization state is qualitatively the same for all wavelengths, thus confirming a reasonably uniform spectral retardance of the equivalent retarder in the displayed spectral range. Quantifying the degree of control of the polarization state

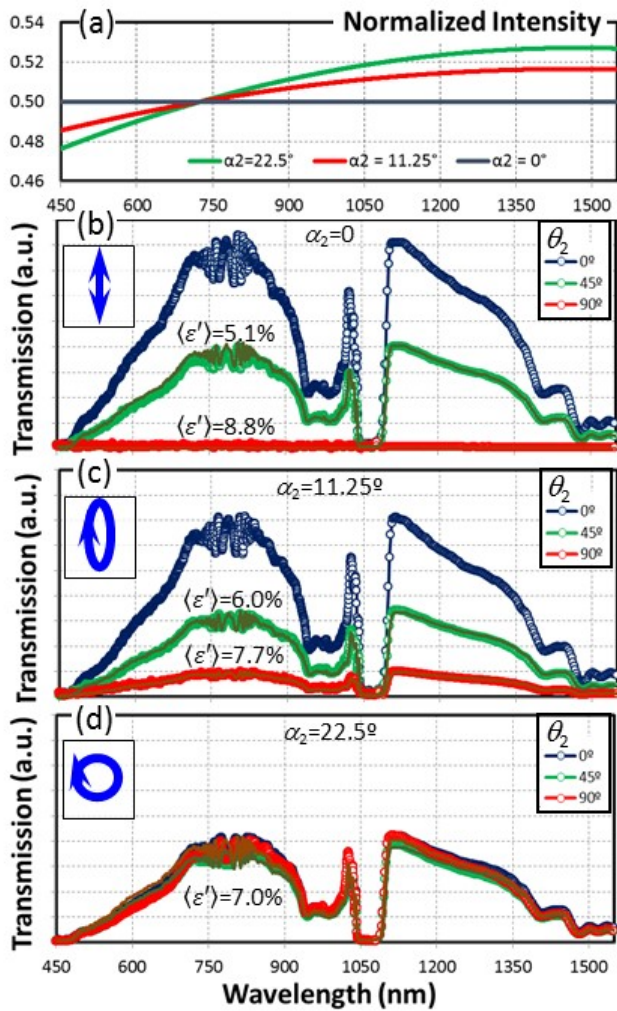


Fig. 3. Spectral transmission of the linear retarder system in Fig. 1 built with FRs. (a) Simulated transmission considering the FR retardance dispersion and a flat input spectrum for the given α_2 and polarizers oriented at $\theta_1=0^\circ$ and $\theta_2=45^\circ$. (b)-(d) Experimental transmission and simulation considering the spectrum of the light source for the given α_2 and polarizers oriented at $\theta_1=0^\circ$ and $\theta_2=0^\circ, 45^\circ$ and 90° .

achieved in this broad spectral range would require polarimetric measurements at various wavelengths. Results in Fig. 3 can be regarded as a proof-of-concept for the tunable broadband linear retarder design. Note that superachromatic QW and HW composite retarders [11, 13] could be fabricated as one piece to build the system in Fig. 1(a) as well.

In conclusion, we have designed a tunable polarization rotator and a tunable linear retarder where the rotation angle and the retardance, respectively, are uniform with wavelength and tunable upon rotating one of the central HWRs. The system can be used to generate a state of polarization that is maintained over a broad spectral range. Of course, the degree of wavelength uniformity of these designs depends on the degree of achromaticity of the optical retarders employed. As a proof-of-concept we show experimental results using FRs, with reasonable uniform retardance in the wide range from 450 to 1550 nm.

The proposed design can find applications whenever a wavelength-uniform retardance other than the standard quarter-

wave and half-wave values are required, or when the required wavelength-uniform retardances need to be tunable. One possible example is the generation of higher-order polarization vector beams by using geometric phase elements like q-plates [27]. The higher-order vector beam generated by these elements depends critically on the input polarization state. The retarder here proposed can be used to tune the same input state of polarization for all wavelengths, thus producing the same higher-order vector beam. We also outline applications in ellipsometry, astronomy and polarimetry, where a tunable wavelength-compensated retarder might be useful to improve current techniques.

Funding. This work was financed by Generalitat Valenciana, Conselleria d'Educació, Investigació, Cultura i Esport (PROMETEO-2017-154) and Ministerio de Economía, Industria y Competitividad of Spain and European Union (MIMECO/FEDER funds, grant FIS2015-66328-C3-3-R). A. Vargas acknowledges support from CONICYT/FONDECYT 1151290.

References

1. D. Goldstein, *Polarized Light*, Taylor and Francis (2011).
2. W. Barbarow, *Photon. Spectra* **43**, 54 (2009).
3. J. Kim, Y. Li, M. N. Miskiewicz, C. Oh, M. W. Kudenov, and M. J. Escuti, *Optica* **2**, 958 (2015).
4. A. Messaadi, M. M. Sánchez-López, P. García-Martínez, A. Vargas, and I. Moreno, *Eur. Opt. Soc. – Rapid Pub.* **12**, 21 (2016).
5. C. M. McIntyre and S. E. Harris, *J. Opt. Soc. Am.* **58**, 1575-1580 (1969).
6. P. Hariharan, *Opt. Eng.* **35**, 3335 (1996).
7. P. Hariharan and P. Ciddor, *J. Mod. Opt.* **51**, 2315 (2004).
8. A. Ardavan, *New. J. Phys.* **9**, 24 (2007).
9. A. Saha, K. Bhattacharya, and A. K. Chakraborty, *Appl. Opt.* **51**, 1976 (2012).
10. S. S. Ivanov, A. A. Rangelov, N. V. Vitanov, T. Peters, and T. Halfmann, *J. Opt. Soc. Am. A* **29**, 265-269 (2012).
11. T. Peters, S. S. Ivanov, D. Englisch, A. A. Rangelov, N. V. Vitanov, and T. Halfmann, *Appl. Optics* **51**, 7466-7474 (2012).
12. T. Mu, C. Zhang, Q. Li, and R. Liang, *Opt. Lett.* **40**, 2485-2488 (2015).
13. J. M. Herrera-Fernández, J. L. Vilas, L. M. Sánchez-Brea, and E. Bernabeu, *Appl. Opt.* **54**, 9758 (2015).
14. R. Desmarchelier, M. Lancry, M. Gecevicius, M. Beresna, P. G. Kazansky, and B. Poumellec, *Appl. Phys. Lett.* **107**, 181111 (2015).
15. E. Dimova, A. Rangelov, and E. Kyoseva, *Photon. Res.* **3**, 177-179 (2015).
16. M. J. Abuleil, and I. Abdulhalim, *Opt. Lett.* **39**, 5487 (2014).
17. I. Moreno, J. V. Carrión, J. L. Martínez, P. García-Martínez, M. M. Sánchez-López, J. Campos, *Opt. Lett.* **39**, 5483 (2014).
18. J. M. Bennett, *Appl. Opt.* **9**, 2123-2129 (1970).
19. D. Mawet, C. Hanot, C. Leanerts, P. Riaud, D. Defrére, D. Vandormael, J. Loicq, K. Fleury, J. Y. Plesseria, J. Surdej, and S. Habraken, *Opt. Express* **15**, 12850 (2007).
20. B. Bakhouché, A. Beniaiche, and H. Guessas, *Opt. Eng.* **53**, 055108 (2014).
21. I. Abdulhalim, *Opt. Commun.* **282**, 3052-3054 (2009).
22. A. Messaadi, A. Vargas, M. M. Sánchez-López, P. García-Martínez, P. Kula, N. Bennis, and I. Moreno, *J. Opt.* **19**, 045703 (2017).
23. K. B. Rochford, A. H. Rose, P. A. Williams, C. M. Wang, I. G. Clarke, P. D. Hale, and G. W. Day, *Appl. Opt.* **36**, 6458-6465 (1997).
24. https://www.thorlabs.com/newgroupage9.cfm?objectgroup_id=154
25. C. Ye, *Opt. Eng.* **34**, 3031 (1995).
26. J. A. Davis, D. E. McNamara, D. M. Cottrell, and T. Sonehara, *Appl. Opt.* **39**, 1549 (2000).
27. Y. S. Rumala, G. Milione, T. A. Nguyen, S. Pratavieira, Z. Hossain, D. Nolan, S. Slussarenko, E. Karimi, L. Marrucci, and R. R. Alfano, *Opt. Lett.* **38**, 5083 (2013).

References (complete record)

1. D. Goldstein, *Polarized Light*, Taylor and Francis (2011).
2. W. Barbarow, "A wave plate for every application", *Photon. Spectra* **43**, 54 (2009).
3. J. Kim, Y. Li, M. N. Miskiewicz, C. Oh, M. W. Kudenov, and M. J. Escuti, "Fabrication of ideal geometric-phase holograms with arbitrary wavefronts", *Optica* **2**, 958 (2015).
4. A. Messaadi, M. M. Sánchez-López, P. García-Martínez, A. Vargas, and I. Moreno, "Optical system for measuring the spectral retardance function in an extended range", *J. Eur. Opt. Soc. – Rapid Pub.* **12**, 21 (2016).
5. C. M. McIntyre and S. E. Harris, "Achromatic wave plates for the visible spectrum", *J. Opt. Soc. Am.* **58**, 1575-1580 (1969).
6. P. Hariharan, "Achromatic and apochromatic half wave and quarter wave retarders", *Opt. Eng.* **35**, 3335 (1996).
7. P. Hariharan and P. Ciddor, "Broad-band superachromatic retarders and circular polarizers for the UV, visible and near infrared", *J. Mod. Opt.* **51**, 2315 (2004).
8. A. Ardavan, "Exploiting the Poincaré–Bloch symmetry to design high-fidelity broadband composite linear retarders", *New. J. Phys.* **9**, 24 (2007).
9. A. Saha, K. Bhattacharya, and A. K. Chakraborty, "Achromatic quarter-wave plate using crystalline quartz", *Appl. Opt.* **51**, 1976 (2012).
10. S. S. Ivanov, A. A. Rangelov, N. V. Vitanov, T. Peters, and T. Halfmann, "Highly efficient broadband conversion of light polarization by composite retarders", *J. Opt. Soc. Am. A* **29**, 265-269 (2012).
11. T. Peters, S. S. Ivanov, D. Englisch, A. A. Rangelov, N. V. Vitanov, and T. Halfmann, "Variable ultrabroadband and narrowband composite polarization retarders", *Appl. Opt.* **51**, 7466-7474 (2012).
12. T. Mu, C. Zhang, Q. Li, and R. Liang, "Achromatization of waveplate for broadband polarimetric system", *Opt. Lett.* **40**, 2485-2488 (2015).
13. J. M. Herrera-Fernández, J. L. Vilas, L. M. Sánchez-Brea, and E. Bernabeu, "Design of superachromatic quarter-wave retarders in a broad spectral range", *Appl. Opt.* **54**, 9758 (2015).
14. R. Desmarchelier, M. Lancry, M. Gecevicius, M. Beresna, P. G. Kazansky, and B. Poumellec, "Achromatic polarization rotator imprinted by ultrafast laser nanostructuring in glass", *Appl. Phys. Lett.* **107**, 181111 (2015).
15. E. Dimova, A. Rangelov, and E. Kyoseva, "Tunable bandwidth optical rotator", *Photon. Res.* **3**, 177-179 (2015).
16. M. J. Abuleil, and I. Abdulhalim, "Tunable achromatic liquid crystal waveplates", *Opt. Lett.* **39**, 5487 (2014).
17. I. Moreno, J. V. Carrión, J. L. Martínez, P. García-Martínez, M. M. Sánchez-López, J. Campos, "Optical retarder system with programmable spectral retardance", *Opt. Lett.* **39**, 5483 (2014).
18. J. M. Bennett, "A critical evaluation of rhomb-type quarterwave retarders", *Appl. Optics* **9**, 2123-2129 (1970).
19. D. Mawet, C. Hanot, C. Leunerts, P. Riaud, D. Defrére, D. Vandormael, J. Loicq, K. Fleury, J. Y. Plessier, J. Surdej, and S. Habraken, "Fresnel rhombs as achromatic phase shifters for infrared nulling interferometry", *Opt. Express* **15**, 12850 (2007).
20. B. Bakhouché, A. Beniaiche, and H. Guessas, "Method for determining the reflection-induced retardance of the Fresnel rhomb", *Opt. Eng.* **53**, 055108 (2014).
21. I. Abdulhalim, "Polarization independent birefringent Fabry-Perot etalon having polarization conversion mirrors", *Opt. Commun.* **282**, 3052-3054 (2009).
22. A. Messaadi, A. Vargas, M. M. Sánchez-López, P. García-Martínez, P. Kula, N. Bennis, and I. Moreno, "Solc filters in a reflective geometry", *J. Opt.* **19**, 045703 (2017).
23. K. B. Rochford, A. H. Rose, P. A. Williams, C. M. Wang, I. G. Clarke, P. D. Hale, and G. W. Day, "Design and performance of a stable linear retarder", *Appl. Opt.* **36**, 6458-6465 (1997).
24. https://www.thorlabs.com/newgrouppage9.cfm?objectgroup_id=154
25. C. Ye, "Construction of an optical rotator using quarter-wave plates and an optical retarder", *Opt. Eng.* **34**, 3031 (1995).
26. J. A. Davis, D. E. McNamara, D. M. Cottrell, and T. Sonehara, "Two-dimensional polarization encoding with a phase-only liquid-crystal spatial light modulator", *Appl. Opt.* **39**, 1549 (2000).
27. Y. S. Rumala, G. Milione, T. A. Nguyen, S. Pratavieira, Z. Hossain, D. Nolan, S. Slussarenko, E. Karimi, L. Marrucci, and R. R. Alfano, "Tunable super-continuum light vector vortex beam generator using a q-plate", *Opt. Lett.* **38**, 5083 (2013).